Journal of Chemical Health Risks

www.jchr.org

JCHR (2026) 16(1), 875-896 | ISSN:2251-6727

Bioremediation Potential of Chromium-Resistant *Paenibacillus taichungensis* Strain MAHA-MIE: Optimization and Characterization Studies

Maha Obaid Al-Osaimi[1,5*], Mohd Izuan Effendi Halmi[1*], Siti Salwa Abd Gani[2†], Khairil Mahmud[3†] and Mohd Yunus Abd Shukor[4†]

[1] Department of Land Management, Faculty of Agriculture, Universiti Putra Malaysia, 43400 Serdang, Selangor, Malaysia.

[2*] Department of Agricultural Technology, Faculty of Agriculture, Universiti Putra Malaysia, 43400 Serdang, Selangor, Malaysia.

[3]Department of Crop Science, Agricultural Technology, Faculty of Agriculture, Universiti Putra Malaysia, 43400 Serdang, Selangor, Malaysia.

[4] Department of Biochemistry, Faculty of Biotechnology and Biomolecular Sciences, Universiti Putra Malaysia, 43400 Serdang, Selangor, Malaysia.

[5] Department of Biology, Turabah University College, Taif University, 26571, Turabah, Taif, Kingdome of Saudia Arabia.

(Received: 10 November 2025 Revised: 23 December 2025 Accepted: 05 January 2026)

KEYWORDS

Bioremediation, Hexavalent Chromium (Cr(VI)), Resistant, Optimisation.

ABSTRACT:

Aim: This study investigated the bioremediation potential of P. taichungensis strain MAHA-MIE-Cr(VI)-resistant bacterium, through systematic screening, biochemical and molecular characterisation, and optimisation of operational conditions.

Methods: The approach involved isolating and identifying Cr(VI)-resistant bacteria through 16S RNA sequencing, followed by optimisation of hexavalent chromium Cr(VI) bioreduction using response surface methodology integrated with artificial neural network (RSM–ANN) modelling. The effects of three independent variables: nutrient broth concentration, pH and Cr(VI) concentration on bioreduction efficiency were examined.

Results: Among thirty-one Cr(VI)-resistant isolates obtained from contaminated soil, strain Cr-RB18 exhibited the highest Cr(VI) reduction capacity. Biochemical analysis characterised the isolate as Gram-variable, facultatively anaerobic, motile, catalase-positive, capable of hydrolysing starch and producing H_2S. Molecular identification confirmed it as P. taichungensis strain MAHA-MIE. Under ANN-optimal conditions—9.56 g/L nutrient broth concentration, pH 6.48, and 69.57 ppm Cr(VI), the strain achieved a maximum Cr(VI) reduction of 99.17%. The model exhibited excellent predictive accuracy, with $R^2 = 0.99$, RMSE = 1.00, SEP = 1.56%, and RPD = 0.63%.

Conclusion: These findings highlight strain MAHA-MIE as a promising candidate for bioremediation of Cr(VI)-contaminated environments, warranting further investigation for field-scale application.

1. Introduction

Cr(VI) is an inherently lethal contaminant due to its carcinogenic, mutagenic, and strong oxidizing properties (Wei et al., 2022). However, Cr(VI) compounds are extensively employed in industrial processes such as electroplating, leather tanning, and textile dyeing (Kao et al., 2021). Due to its non-biodegradable nature and continuous release, it persists in the environment and accumulates in the food chain, posing a serious threat to ecosystems and underscoring the urgent need for effective and safe reduction techniques (Yu et al., 2022). The remediation methods for Cr(VI) contamination

Journal of Chemical Health Risks
www.jchr.org
JCHR (2026) 16(1), 875-896 | ISSN:2251-6727

primarily include conventional methods such as chemical reduction, precipitation, flotation, solvent extraction, and various membrane-based techniques are often costly, inefficient, and non-selective, and may generate secondary pollutants (Anderson et al., 2022; Ukhurebor et al., 2021). Duo to these limitations, attention has increasingly shifted toward more sustainable alternatives, with biological remediation emerging as a promising and environmentally friendly option for heavy metal removal (Elahi et al., 2020; Nacer et al., 2021).

Bioremediation is a biological process that minimises the severity of pollutants by degrading or removing complex toxic compounds and converting them into less toxic forms with the mediation of biological agents (Ajona & Vasanthi, 2021). The microbial approach offers several advantages including rapid growth rates, low operational cost, minimal energy requirements, and adaptability to harsh environmental conditions (Jobby et al., 2018).

The optimization of bioremediation processes is critical for improving efficacy while minimizing cost and complexity. Conventional "one-variable-at-a-time" (OVAT) methods require an increased number of experimental runs, are inefficient, and often fail to account for interactive effects among multiple process variables (Abdel-Fattah et al., 2005; Baş & Boyacı, 2007). In contrast, multivariate techniques such as Response Surface Methodology (RSM) enable empirical modelling and optimization of bioprocesses by fitting linear or quadratic polynomial equations to experimental data, thereby facilitating the identification of optimal conditions with fewer experimental runs (Bezerra et al., 2008; Teófilo & Ferreira, 2006). More recently, artificial intelligence approaches particularly ANNs have become prevalent in bioprocess optimisation. ANNs emulate biological learning systems and are particularly effective at capturing complex, non-linear relationships between input variables and response outputs. Their self-learning capabilities and superior predictive accuracy make them valuable tools for modelling and enhancing microbial remediation systems (Alam et al., 2022; Lakshmi et al., 2021; Manohar & Divakar, 2005; Shet et al., 2018). The present study aimed to isolate, identify, and characterise a Cr(VI)-resistant bacterial strain from industrially contaminated soils. The Cr(VI) bioreduction capacity of the isolate was assessed and subsequently optimised using both RSM and ANN models, focusing on three independent variables: nutrient broth concentration, pH, and Cr(VI) concentration. The strain, designated MAHA-MIE, is hypothesised to possess natural adaptive mechanisms for Cr tolerance, making it a compelling candidate for practical, field-scale applications in the bioremediation of Cr(VI)-contaminated environments.

2. Materials and Methods

2.1 Chemicals and Materials

All reagents utilised were of analytical grade and procured from Sigma-Aldrich (St. Louis, MO, USA), Fisher Scientific (Malaysia), and Merck (Darmstadt, Germany). Prior to use, glassware was acid-washed with 10% (v/v) nitric acid (HNO_3) and subsequently rinsed twice with deionised water to remove residual residual trace metals. All culture media, both liquid and solid, were sterilised via autoclaving at 121 °C for 15 minutes. Potassium dichromate ($K_2Cr_2O_7$) was used as the source of Cr(VI) in all relevant assays.

2.3 Isolation of Cr(VI)-Reducing Bacteria

The samples were collected from soil (0–10 cm depth) using a soil auger from various sites in Selangor, Malaysia. The samples were preserved in sterilised Falcon™ tubes following standard microsampling protocols and were immediately transported to the laboratory for further analysis. Ten grams of soil sample were inoculated into 90 mL of nutrient broth (NB) and incubated overnight at 170 rpm at room temperature. Subsequently, the broth culture was serially diluted to a 10^{-5} dilution, and 100 µL was spread onto nutrient agar plates enriched with 50 ppm $K_2Cr_2O_7$, then incubated for 24 hours (Ram Talib et al., 2019). Isolates exhibiting homogeneous morphological characteristics were picked and re-streaked onto the same medium, followed by incubation for 24 hours to obtain purified single colonies.

2.4 Primary and Secondary Screening of Cr(VI)-Reducing Bacteria

For the primary screening of hexavalent chromium [Cr(VI)]-bioreducing bacteria, 100 µL of the overnight culture was added to 10 mL of nutrient broth enriched with 50 ppm $K_2Cr_2O_7$. The liquid medium was then incubated at 170 rpm at room temperature for 24 hours. The supernatant obtained from 1 mL of culture,

Journal of Chemical Health Risks
www.jchr.org
JCHR (2026) 16(1), 875-896 | ISSN:2251-6727

centrifuged at 10,000 × g for 10 minutes, was used to measure the Cr(VI) reduction rate using the 1,5-diphenylcarbazide colorimetric method. For this step, 400 µL of the bacterial culture supernatant, 400 µL of 1 N sulfuric acid (H_2SO_4), and 200 µL of 1,5-diphenylcarbazide reagent were mixed. The reaction mixture was allowed to stand at room temperature for colour development, and the OD_{540} nm was measured using an ultraviolet–visible spectrophotometer (Shimadzu UV–Vis spectrophotometer, Japan) (Sopian et al., 2014). The Cr(VI) reduction rate was calculated as a percentage using Equation (1) (Khanam et al., 2024):

$$Reduction\ Cr(VI)\ rate\ (\%) = \frac{Absorbance\ of\ control + Absorbance\ of\ sample}{Absorbance\ of\ control} \quad (1)$$

For the secondary screening, the bacterial isolates that showed the highest Cr(VI) reduction rate were selected and screened at 100 ppm $K_2Cr_2O_7$ using the same procedures as previously described.

2.5 Morphological and Biochemical Characterisation of Cr(VI)-Reducing Isolates

The colony morphology of the candidate isolate, including surface texture, pigmentation, margin, size, and elevation, was recorded on nutrient agar plates. Biochemical characterisation was performed through Gram staining, catalase testing, hydrogen sulphide (H_2S) production, motility assays, indole production, and starch hydrolysis, as described in standard protocols (Abbas, 2023; Firdausi et al., 2024; Masi et al., 2021).

2.6 Molecular Identification via 16S rRNA Sequencing

Genomic DNA of the candidate bacterial isolate was extracted by Apical Scientific Sdn. Bhd., Selangor, Malaysia, using the Bacterial DNA Barcoding Kit (1st BASE, Malaysia), and the full-length 16S rRNA gene (~1500 bp) was amplified with universal primers 27F and 1492R. The PCR amplicons were verified by agarose gel electrophoresis, purified, and sequenced. The resulting sequences were analysed using BLAST to determine the closest phylogenetic matches, and a phylogenetic tree was constructed in MEGA (version 11.0.13) using the Neighbor-Joining method (Prashanthi et al., 2021).

2.7 Effect of Cr(VI) Concentration on Bacterial Growth

The effect of varying Cr(VI) concentrations on bacterial proliferation was assessed by inoculating 100 µL of overnight culture into 10 mL of NB containing 0, 25, 50, 100, 150, and 200 ppm $K_2Cr_2O_7$. Cultures were incubated at 170 rpm at room temperature, and 1 mL samples were withdrawn at 4-hour intervals for 24 hours. Each sample was centrifuged at 10,000 × g, and the optical density of the supernatant was measured at 600 nm (OD_{600}). Simultaneously, Cr(VI) reduction was assessed using the colourimetric assay described earlier. Bacteria-free LB medium containing equivalent Cr(VI) concentrations was used as the negative control (Ram Talib et al., 2019).

2.8 Effect of Hexavalent Chromium Cr(VI) on Bacterial Cell Growth

According to Ram Talib et al. (2019), with minor modifications, 100 µL of the overnight culture was inoculated into each concentration of $K_2Cr_2O_7$ in NB (0, 25, 50, 100, 150, and 200 ppm). The NB flasks were then incubated at 170 rpm at room temperature. Every 4 hours, from the start of the experiment until 24 hours of incubation, 1 mL of the sample was centrifuged at 10,000 × g for 10 minutes. The bacterial pellet was resuspended in sterile 0.085% NaCl solution, and the growth rate was measured at OD_{600} every 4 hours. The Cr(VI) reduction rate at each concentration was measured using the supernatant every 4 hours, as described in Section 2.4. Bacteria-free media supplemented with the same concentrations used in the experimental groups were used as the controls (Ram Talib et al., 2019).

2.9 Optimization via Response Surface Methodology (RSM)

The experiment was designed using the Box–Behnken Design (BBD) to identify the optimal levels of significant factors for maximum Cr(VI) reduction (Box & Behnken, 1960). The minimum and maximum responses for three independent variables (nutrient broth concentration, pH, and Cr(VI) concentration) are shown in Table 1.

Journal of Chemical Health Risks
www.jchr.org
JCHR (2026) 16(1), 875-896 | ISSN:2251-6727

Table 1 Coded and actual values of independent variables used in Box–Behnken design.

Independent Variables	Unit	Level		
		-1	0	+1
pH	g/L	6	6.75	7.5
Nutrient Broth conc.	-	3	6.5	10
Cr(VI) conc.	ppm	50	75	100

Design-Expert® software (version 13) was used to design the matrix and perform statistical calculations. All 17 experimental runs were conducted under the conditions outlined in Table 2 to determine the effects of three experimental factors (nutrient broth concentration, pH, and Cr(VI) concentration) on the experimental response (Cr(VI) reduction rate). A total of 100 µL of the overnight culture was inoculated into 10 mL of NB and incubated under shaking conditions at 170 rpm at room temperature for 24 hours. The Cr(VI) reduction rate was measured using the supernatant (1 mL) obtained after centrifugation at 10,000 × g for 10 minutes, as described in Section 2.4. Statistical analysis of the experimental data was conducted to evaluate the significance of the regression and the fitted model through an ANOVA test. Key statistical parameters (F-value, P > F, Lack of Fit, and both predicted and adjusted R^2 values) were computed to assess model performance (Bezerra et al., 2008).

Table 2 Experimental design matrix.

Run	Independent Variables		
	Nutrient Broth Conc. (g/L)	pH	Cr(VI) Conc. (ppm)
1	6.5	7.5	50
2	10	6	75
3	6.5	6.75	75
4	10	6	50
5	10	6.75	100
6	3	6	75
7	6.5	6.75	75
8	6.5	6	100
9	10	6.75	50
10	3	7.5	75
11	6.5	6.75	75
12	3	6.75	50
13	6.5	6.75	75
14	6.5	7.5	100
15	6.5	6.75	75
16	3	6.75	100
17	10	7.5	75

2.9 Optimization Using Artificial Neural Networks (ANN)

The derived datasets from the BBD matrix were used for developing a predictive model with Neural Power version 2.5. (CPC-X Software, USA). The data were randomly divided into two sets: the training dataset was used to minimise the error and determine the model parameters, while the testing dataset was used to evaluate the trained model (Saber et al., 2023). The ANN topology was designated as 3-X-1. Three neurons of the independent variables (i.e., nutrient broth concentration, pH, and Cr(VI) concentration) represent the input layer. The output layer is composed of one neuron (Cr(VI) reduction rate). A hidden layer was added between the input and output layers, in which a range of neurons from 3 to 15 was tested to determine the ideal number of neurons in this layer. ANN was trained using a trial-and-error approach, taking into account parameters such as the learning algorithm, the optimal number of neurons in the hidden layer, the number of hidden layers, and the transfer function (Gendy et al., 2021), allowing the model to adjust interconnection weights and determine the appropriate number of hidden-layer neurons needed to minimise the difference between predicted and experimental values (Kothari et al., 2022). The trial-and-error process was used until the lowest error was achieved, with a root mean square error (RMSE) < 0.01 and an average correlation coefficient (R) ≈ 1. The coefficient of determination (R^2) ≈ 1 between the predicted and actual values was also used to evaluate the

Journal of Chemical Health Risks
www.jchr.org
JCHR (2026) 16(1), 875-896 | ISSN:2251-6727

training process (Ram Talib et al., 2019; Saber et al., 2023).

2.10 Identification of Optimum Conditions via RSM and ANN

The optimum points for the reduction of Cr(VI) via *P. taichungensis* strain MAHA-MIE were determined using the fitted models of both RSM and ANN. The desirability function, through numerical optimisation in Design-Expert® software (version 13), was used to identify the optimum points in the RSM model. Meanwhile, a genetic algorithm was used to calculate the optimum points in the ANN model using Neural Power version 2.5 (CPC-X Software, USA). The predicted optimum conditions from the RSM and ANN models were validated, and the standard deviation was calculated to evaluate the accuracy of both models (Ram Talib et al., 2019).

2.11 Comparison of RSM and ANN Performance

The following statistical parameters were computed between actual data and predicted values for both RSM and ANN models to compare the analysis of error. Equations (2), (3), (4), and (5) were used:

$$\boldsymbol{RMSE = \sqrt{\frac{\sum_{i=1}^{n}\left(Y_{i.p} - Y_{i.e}\right)^2}{n}}} \qquad (2)$$

$$\boldsymbol{R^2 = 1 - \frac{\sum_{i=1}^{n}\left(Y_{i.p} - Y_{i.e}\right)^2}{\sum_{i=1}^{n}\left(Y_{i.p-Y_e}\right)^2}} \qquad (3)$$

$$\boldsymbol{SEP = \frac{RSME}{Y_e} \times 100} \qquad (4)$$

$$\boldsymbol{RPD = \frac{100}{n}\sum_{i=1}^{n}\frac{\left|\left(Y_{I.e} - Y_{i-p}\right)\right|}{\left|\left(Y_{i.e}\right)\right|}} \qquad (5)$$

In these equations, RMSE denotes the root mean square error, R^2 represents the coefficient of determination (correlation coefficient), SEP refers to the standard error of prediction, RPD signifies the relative percent deviation, $Y_{(i\cdot e)}$ indicates the experimentally observed response, $Y_{(i\cdot p)}$ denotes the predicted value, Y_e is the mean of the observed responses, and n corresponds to the total number of experimental runs. In this context, lower values of RMSE, SEP, and RPD, combined with higher R^2 values reflect superior model accuracy and enhanced predictive performance (Yang et al., 2022).

3.9 Studying the Effect of Cr(VI) on the Cellular Morphology of Free Cells of *P. taichungensis* strain MAHA-MIE Using SEM

According to Maurya et al. (2022), with some modifications, 100 µL of the overnight culture was inoculated into 10 mL NB medium at three different concentrations of $K_2Cr_2O_7$ (0, 50, and 100 ppm), and incubated for 24 hours at 170 rpm. The isolate was harvested by centrifugation, and the bacterial pellets were then fixed with 2.5% (w/v) glutaraldehyde overnight at 4 °C. The pellets were washed twice with phosphate-buffered saline (PBS, pH ~7.4) to remove any excess fixative. Following fixation, the cells were dehydrated using ethanol with progressively increasing concentrations of 30%, 50%, 70%, 90%, 95%, and 100%, each for 10 minutes, and were then gold-coated and examined under a scanning electron microscope (SEM) (SEM; JSM-6400, JEOL, Japan) (Maurya et al., 2022).

3 Results and Discussion

3.1 Isolation and and Screening of Cr(VI)-Reducing Bacteria

Bacterial resistance remains a crucial preliminary criterion for evaluating strains with potential Cr(VI)-reduction capability (Narayani & Shetty, 2013). For a preliminary screening of the Cr(VI)-reducing capability, thirty-one bacterial isolates were inoculated into a broth medium containing 50 ppm of Cr(VI) and incubated for 24 hours. All isolates showed varying percentages of Cr(VI)-reducing activity (Fig. 1). The isolated Cr(VI)-reducing bacteria (Cr-RB) were designated Cr-RB1 to Cr-RB31. Among these, isolates Cr-RB5, Cr-RB18, Cr-RB22, Cr-RB24, Cr-RB28, and Cr-RB30 demonstrated the highest reduction efficiencies, each achieving over 85% reduction of Cr(VI). These findings align with previous reports documenting the isolation of Cr(VI) -tolerant bacteria from tannery and industrial effluents capable of reducing Cr(VI) at concentrations exceeding 40 mg/L (Farag & Zaki, 2010; Mustapha & Halimoon, 2015).

Journal of Chemical Health Risks
www.jchr.org
JCHR (2026) 16(1), 875-896 | ISSN:2251-6727

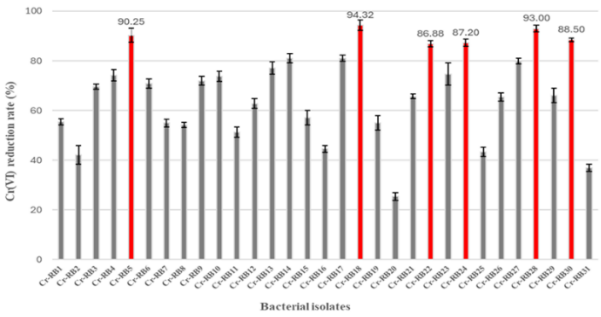

Fig. 1 Primary screening of Cr(VI)-reducing bacteria at 50 ppm $K_2Cr_2O_7$. Data are presented as the mean of triplicate samples ± standard error.

To evaluate their performance under more environmentally realistic conditions, these six isolates were subjected to secondary screening at an elevated Cr(VI) concentration of 100 ppm (Dakiky et al., 2002). the bacterial isolate Cr-RB18 exhibited the highest reduction efficiency, achieving 90.34% removal of Cr(VI) (Fig. 2). This observation aligns with the findings of Meng et al. (2020), who reported that the isolate CRB6 achieved reduction efficiencies approaching 98% (Meng et al., 2022). Similar results have also been documented for strains derived from industrial wastewaters, where tolerance thresholds up to 100 mg/L were observed (Kalsoom et al., 2021). Bacterial strains demonstrating elevated tolerance to Cr(VI) generally exhibit enhanced bioreductive capacity, effectively converting Cr(VI) to its less toxic trivalent form Cr(III), thereby reinforcing their potential as viable agents for the bioremediation of Cr-contaminated environments (Sanjay et al., 2020). Thus, Cr-RB18 was selected for further study as a potential candidate for Cr(VI) bioremediation.

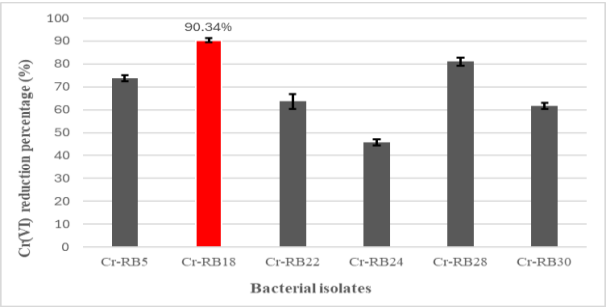

Fig. 2 Secondary screening of Cr(VI)-reducing bacteria at 100 ppm $K_2Cr_2O_7$. Data are presented as the mean of triplicate samples ± standard error.

3.2 Morphological and and Biochemical Characterisation of Cr(VI)-Reducing Isolate Cr-RB18

The bacterial isolate Cr-RB18 was obtained from the surrounding soil near an industrial facility within the Kawasan Perindustrian Seri Kembangan, Selangor, Malaysia (3°01.738′ N, 101°71.233′ E). Soil microbial communities in such environments often develop adaptive mechanisms to cope with heavy metal stress. Chromium contamination disrupts elemental cycling and microbial dynamics, as microorganisms are compelled to divert metabolic energy towards stress mitigation and cellular repair. Nevertheless, many bacteria have evolved detoxification strategies that enable survival and functional activity under Cr(VI) stress, rendering them promising candidates for bioremediation applications (Ahmad et al., 2022; Newsome & Falagán, 2021).

The colonies of Cr-RB18 are small, circular, and greyish-white, with undulate margins, flat elevation, and a smooth surface. Biochemical tests revealed that the strain is Gram-variable, motile, facultatively anaerobic, catalase-positive, capable of hydrolysing starch, and produces hydrogen sulphide (H_2S).

Since the study by Romanenko and Koren'Kov (1977), which first demonstrated the Cr(VI)-reducing capability of Pseudomonas sp., the ability of bacteria to reduce Cr(VI) has been documented across a wide range of aerobic and anaerobic species (Ahmad et al., 2022), such as *K. pneumoniae* and *B. altitudinis* isolated from bauxite mining areas (AMELIA et al., 2023), *Microbacterium paraoxydans* from tannery effluents (Mishra et al., 2021), and *B. vallismortis, B. haynesii,* and *A. aquatilis* from tannery sludge (Maurya et al., 2022).

3.3 Molecular Identification of Cr(VI)-Reducing Bacteria

Molecular identification based on 16S rRNA gene sequencing offers superior taxonomic resolution compared to conventional biochemical profiling, particularly when characterising environmental isolates with potentially novel phenotypes (Sanjay et al., 2020). To accurately classify isolate Cr-RB18, genomic DNA was extracted and the 16S rRNA gene was amplified using universal primers 27F (5′-AGAGTTTGATCCTGGCTCAG-3′) and 1492R (5′-

Journal of Chemical Health Risks
www.jchr.org
JCHR (2026) 16(1), 875-896 | ISSN:2251-6727

GGTTACCTTGTTACGACTT-3′) (Dos Santos et al., 2019; Heuer et al., 1997).

BLAST analysis of the sequenced fragment against the NCBI GenBank database revealed 100% sequence identity with *Paenibacillus taichungensis*, 95% identity with *P. pabuli*, and 73% with *P. barcinonensis*. These results unambiguously assign Cr-RB18 to the genus *Paenibacillus*, with the highest degree of similarity to *P. taichungensis*. Phylogenetic reconstruction was conducted using MEGA software version 11.0.13, applying the Neighbor-Joining algorithm with 100 bootstrap replications to assess clade stability. As shown in Fig. 3, Cr-RB18 clustered robustly with reference sequences of *P. taichungensis*, supported by a bootstrap value of 100%, indicating strong genetic relatedness. *Salmonella enterica* was included as an outgroup to root the tree and to underscore the phylogenetic distinction between the *Paenibacillus* lineage and other genera.

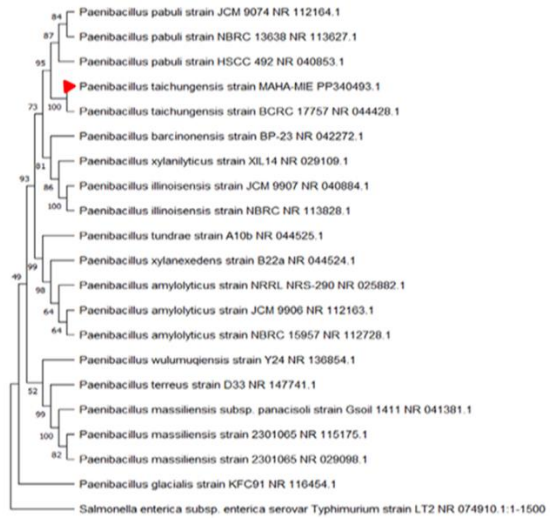

Fig. 3: Phylogenetic tree showing the relationship of strain MAHA-MIE (PP340493.1) to related species. A 100% bootstrap value confirms its close affinity to *P. taichungensis* BCRC 17757.

3.4 Screening of Media for Cr(VI) Bioreduction by Strain MAHA-MIE

The selection of an appropriate culture medium is critical in microbial bioremediation studies given the capacity of microorganisms to tolerate and adapt to diverse growth conditions (Navarrete-Perea et al., 2021). Strain MAHA-MIE was cultivated in three media namely nutrient broth (NB), Luria-Bertani (LB), and minimal salt medium (MSM) to assess their influence on Cr(VI) reduction efficiency. These media provide the essential nutrients required for bacterial survival, growth, and metabolic activity (Madhavi et al., 2013)

After 24 hours of incubation, NB supported the highest Cr(VI)-reduction efficiency at 93.28%, followed by LB medium at 85.85%, while MSM exhibited the lowest performance at 57.65% (Fig. 4). Comparable outcomes were reported for *A. radioresistens* strain NS-MIE, which exhibited high Cr(VI)-reduction efficiency in nutrient broth (NB) compared to Luria–Bertani (LB) and minimal salt medium (MSM) (Ram Talib et al., 2019). Similarly, Meng et al. (2022) reported that isolate CRB6 achieved 98% Cr(VI) reduction in NB (Meng et al., 2022).

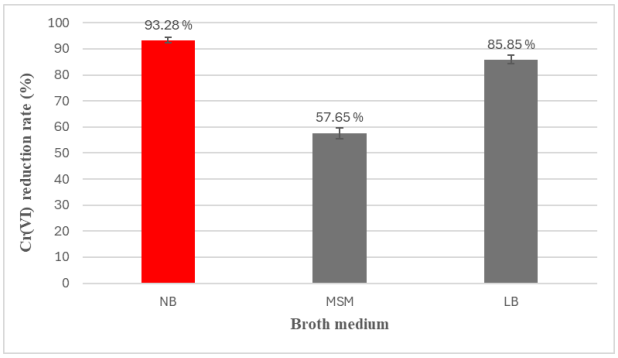

Fig. 4: Screening of Media for Cr(VI) Bioreduction

3.5 Effect of Cr(VI) on the Growth Dynamics of Strain MAHA-MIE

The growth response of strain MAHA-MIE to varying Cr(VI) concentrations (0, 25, 50, 100, 150, and 200 ppm) was evaluated by monitoring optical density (OD_{600}) at 4-hour intervals over 24 hours (Fig. 5). Growth remained comparable to the control at 25 ppm and 50 ppm, indicating minimal inhibitory effects and strong physiological tolerance to Cr(VI). This resilience is likely associated with intrinsic detoxification mechanisms, such as exopolysaccharide (EPS)-mediated metal sequestration, chemical neutralisation, and efflux-based resistance systems (Akhzari et al., 2024; Zeng et al., 2020). However, a critical growth inhibition threshold was evident at 100 ppm Cr(VI), beyond which pronounced toxicity became apparent. Marked suppression of cellular proliferation occurred at 150 and 200 ppm, indicating that the upper tolerance limit had

Journal of Chemical Health Risks
www.jchr.org
JCHR (2026) 16(1), 875-896 | ISSN:2251-6727

been exceeded under these concentration (Rath et al., 2014).

Comparable growth inhibition trends at elevated Cr(VI) levels have been reported for *Bacillus velezensis* (Bao et al., 2023), *Bacillus sp.* CRB-B1 (Tan et al., 2020), and *Sporosarcina saromensis* W5 (Huang et al., 2021). Notably, detectable growth even at 200 ppm after 24 hours reflects the isolate's intrinsic resistance, underscoring its potential utility in bioremediation of Cr(VI)-contaminated environments.

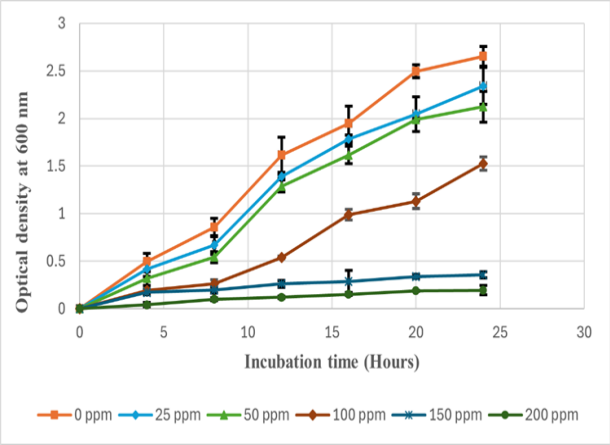

Fig. 5: Growth rate of strain MAHA-MIE at different concentrations of Cr(VI)

Fig. 7 displays the Cr(VI) reduction efficiency of strain MAHA-MIE across the same Cr(VI) concentration range. The optimal reduction was achieved at 24 hours, with ≥ 90% reduction efficiency observed at 25, 50, and 100 ppm. During the logarithmic phase of bacterial growth, over 60% of Cr(VI) was reduced (Mishra et al., 2021). In this phase, bacteria reduced Cr(VI) significantly better (Ikegami et al., 2020), likely driven by heightened enzymatic activity associated with active metabolism. In contrast, higher Cr(VI) concentrations were associated with diminished reduction rates and required extended incubation for effective detoxification (Sadhana Sagar et al., 2012).

Similar findings were documented by Bharagava and Mishra (2018), who isolated *Cellulosimicrobium sp.* (KX710177) from tannery effluents. While the isolate reduced 50 mg/L Cr(VI) within 24 hours, 96 hours were required to achieve similar reduction at 100 mg/L (Bharagava & Mishra, 2018).

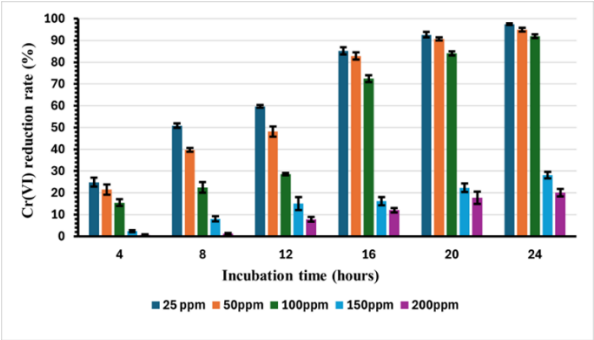

Fig. 6 : Effect of different initial concentration of Cr(VI) on Cr(VI) reduction efficiency (%).

3.6 Optimization of Cr(VI) Reduction via RSM Approach

A quadratic response surface methodology (RSM) model was employed to optimise the Cr(VI) bioreduction efficiency by free cells of the strain MAHA-MIE. Three independent variables, nutrient broth concentration (A), pH (B), and Cr(VI) concentration (C) were investigated, with Cr(VI) reduction rate (Y) as the response. The regression equation (6) derived from the Box–Behnken Design (BBD) is presented as follows:

$$Y=+73.03+19.65A-5.52B-9.11C-2.27AB-5.28AC+2.94BC-18.78A^2-2.20B^2+1.45C^2 \quad (6)$$

In the above equation, Y is the predicted Cr(VI) reduction rate, A is nutrient broth concentration, B is pH, C is Cr(VI) concentration, AB, AC, and BC refer to the interaction effects between nutrient broth concentration and pH, nutrient broth concentration and Cr(VI) concentration, and pH and Cr(VI) concentration, respectively. A^2, B^2, and C^2 denote the quadratic effects of nutrient broth concentration, pH, and Cr(VI) concentration, respectively.

Journal of Chemical Health Risks
www.jchr.org
JCHR (2026) 16(1), 875-896 | ISSN:2251-6727

Table 3. Experimental design matrix showing actual, RSM-predicted, and ANN-predicted values for Cr(VI) reduction efficiency (%).

Run	Independent variables			Cr (VI) reduction %		
	Nutrient broth conc. (g/L)	pH	Cr (VI) conc. (ppm)	Actual values of experiment	Predicted values of RSM	Predicted values of ANNs
1	Tra.6.5	Tra.7.5	Tra.50	Tra.69.57	72.92	69.57
2	Tra.10	Tra.6	Tra.75	Tra.78.42	79.49	78.42
3	Tra.6.5	Tra.6.75	Tra.75	Tra.70.14	73.03	72.91
4	Tra.10	Tra.6	Tra.50	Tra.96.90	98.27	96.91
5	Tra.10	Tra.6.75	Tra.100	Tra.59.53	60.96	59.53
6	Tra.3	Tra.6	Tra.75	Tra.35.07	35.65	35.07
7	Tra.6.5	Tra.6.75	Tra.75	Tra.75.69	73.03	72.80
8	Tra.6.5	Tra.6	Tra.100	Tra.68.76	65.74	68.76
9	Tra.10	Tra.6.75	Tra.50	Tra.93.38	89.74	93.38
10	Tra.3	Tra.7.5	Tra.75	Tra.31.25	29.15	31.25
11	Tra.6.5	Tra.6.75	Tra.75	Tra.73.47	73.03	72.91
12	Tra.3	Tra.6.75	Tra.50	Tra.40.97	39.88	40.97
13	Tra.6.5	Tra.6.75	Tra.75	Tra.72.92	73.03	72.93
14	Tra.6.5	Tra.7.5	Tra.100	Tra.61.62	60.59	61.63
15	Tes.6.5	Tes.6.75	Tes.75	Tes.72.26	73.03	72.93
16	Tes.3	Tes.6.75	Tes.100	Tes.29.60	32.21	29.60
17	Tes.10	Tes.7.5	Tes.75	Tes.64.16	63.92	64.16

Tra. denotes the training dataset, and Tes. denotes the testing dataset, with independent variables as inputs and the percentage of Cr(VI) reduction (%) as the output.

Analysis of variance (ANOVA) was employed to assess the influence of individual and interaction effects of the selected factors—nutrient broth concentration, pH, and Cr(VI) concentration on the bioreduction efficiency of strain MAHA-MIE. ANOVA is a robust statistical method for evaluating model adequacy by partitioning the total variance into components attributed to the model and residual error (Bezerra et al., 2008; Guo et al., 2021). As summarised in Table 4, the fitted quadratic model yielded an F-value of 69.97 and a p-value < 0.0001, confirming the model's high statistical significance. The lack-of-fit p-value (0.0943) exceeded 0.05, indicating that the model sufficiently fits the experimental data without significant systematic deviation (Zaib & Ahmad, 2020).

The model demonstrated excellent predictive performance, with R^2 and adjusted R^2 values of 0.9890 and 0.9749, respectively. The minimal difference between these values (<0.02) suggests that the quadratic model accurately represents the actual response.

Journal of Chemical Health Risks
www.jchr.org
JCHR (2026) 16(1), 875-896 | ISSN:2251-6727

Table 4 Analysis of variance (ANOVA)

Source	Sum of Squares	df	Mean Square	F-value	p-value	
Model	6197.18	9	688.58	69.97	< 0.0001	**significant**
A-Nutrient Broth	3191.57	1	3191.57	324.32	< 0.0001	
B-pH	219.47	1	219.47	22.30	0.0022	
C-Cr (VI) conc.	598.41	1	598.41	60.81	< 0.0001	
AB	21.97	1	21.97	2.23	0.1788	
AC	119.02	1	119.02	12.09	0.0103	
BC	28.42	1	28.42	2.89	0.1330	
A^2	1216.83	1	1216.83	123.65	< 0.0001	
B^2	19.03	1	19.03	1.93	0.2069	
C^2	8.25	1	8.25	0.8384	0.3903	
Residual	68.88	7	9.84			
Lack of Fit	52.76	3	17.59	4.36	0.0943	**not significant**
Pure Error	16.12	4	4.03			
Cor Total	6266.06	16				
					R^2	0.9890
					R^2 adjusted	0.9749

∗P > F less than 0.05 = statistically significant

Moreover, statistical analysis revealed that nutrient broth concentration (A), pH (B), Cr(VI) concentration (C), and their interaction (AC), along with the quadratic term A^2, had significant effects on Cr(VI) reduction ($p < 0.05$). Among these, nutrient broth concentration and Cr(VI) concentration were highly significant ($p < 0.0001$), indicating their dominant influence on the bioreduction efficiency. Other interaction and quadratic terms (AB, BC, B^2, and C^2) were statistically non-significant.

In this study, the Box–Behnken Design (BBD) was successfully employed to optimize the independent variables, achieving the maximum Cr(VI) reduction, where the strain MAHA-MIE exhibited a reduction efficiency of 96.90%. Similarly, the effectiveness of BBD has been reported in studies involving Cr(VI) removal using Fe_3O_4-activated carbon composites (Afshin et al., 2021), melanin biosynthesis (Saber et al., 2023), removal of environmental contaminants using magnetic nanocomposites (Buenaño et al., 2024), and methylene blue adsorption on agricultural solid waste (Dbik et al., 2022). The optimised conditions for Cr(VI) reduction were 10 g/L nutrient broth, pH 6.0, and 50 ppm Cr(VI). Similarly, Ram Talib et al. (2019) also reported an optimum nutrient broth concentration of 10 g/L for *A. radioresistens* NS-MIE (Ram Talib et al., 2019).

The optimal pH of 6.0 corresponds with the preferred growth range (pH 6–8) of *Paenibacillus spp*. (Lee et al., 2008), and supports efficient Cr(VI) reduction by maintaining enzymatic activity and cellular integrity at the optimal pH, whereas extreme pH conditions can inhibit Cr(VI) reduction efficiency (Fito et al., 2023; Huang et al., 2023). Notably, high Cr(VI) concentrations affect cell growth and can disrupt biological activities essential for the reduction process (McLean et al., 2000).

Journal of Chemical Health Risks
www.jchr.org
JCHR (2026) 16(1), 875-896 | ISSN:2251-6727

Fig.7 illustrates several important diagnostic plots used to evaluate the adequacy of the model through residual analysis and to assess the accuracy of the model's fit to the experimental data (Amdoun et al., 2010). The normal probability plot of residuals (Fig. 7a) indicates a near-linear distribution, suggesting residuals are normally distributed. Similarly, the normal probability plot of residuals for aqueous Cr(VI) adsorption onto activated carbon derived from sugar beet bagasse agricultural waste showed a good linear fit (Ghorbani et al., 2020). The residual plots against predicted values and run number (Fig. 7b and 7c) exhibit random scatter within the range of ±4.0, suggesting that the Box-Behnken model effectively established the relationship between the independent variables and Cr(VI) reduction efficiency. Fig.7d illustrates a plot of predicted versus actual values, where the data points are approximately aligned along a straight line, indicating consistent variance and high accuracy in predicting actual values for the RSM model (Mohammadi et al., 2017). This result aligns with findings by Hussain et al. (2020), who observed that actual data for the removal of hexavalent chromium by *Pseudomonas sp.* WS-D/183 aligned closely along predicted line, indicating a good fit for the quadratic model (Hussain et al., 2020)

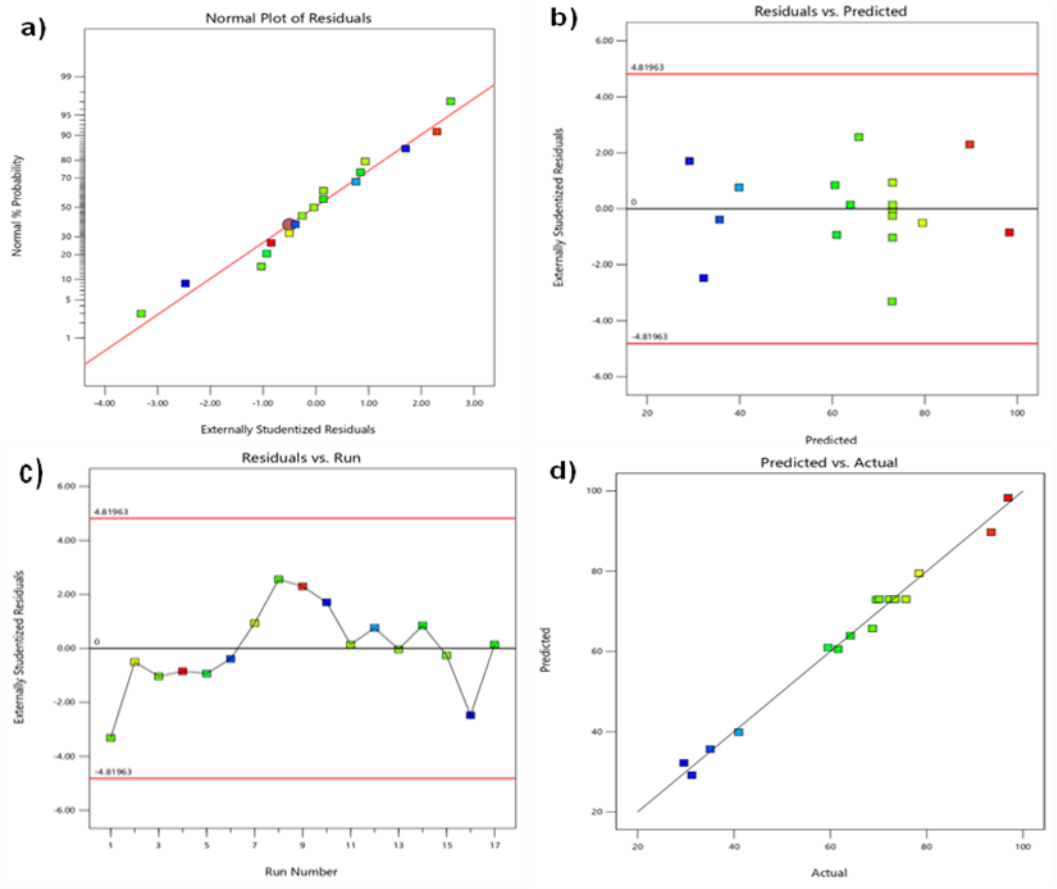

Fig. 7: Diagnostic plots of the quadratic model used in RSM.

3.7 Optimization of Cr(VI) Reduction via ANN Approach

Artificial Neural Networks (ANNs) constitute a class of computational modelling techniques widely employed to characterise complex processes and mathematical constructs. The implementation of ANNs typically encompasses the selection of an appropriate network topology, determination of the optimal number of

Journal of Chemical Health Risks
www.jchr.org
JCHR (2026) 16(1), 875-896 | ISSN:2251-6727

neurons within the hidden layers, execution of the training and learning algorithms, and subsequent validation and verification of the model's predictive performance (Gurney, 2018). ANNs are increasingly employed across various environmental engineering domains, including solid waste management (Nabavi-Pelesaraei et al., 2017), wastewater treatment (Fan et al., 2018), and groundwater contamination (Bayatzadeh Fard et al., 2017).

In this study, a batch back-propagation (BBP) ANN model was developed using a multilayer feedforward network to model and optimise Cr(VI) reduction by strain MAHA-MIE. The input parameters consisted of nutrient broth concentration, Cr(VI) concentration, and pH, while the output parameter was the Cr(VI) reduction efficiency. Based on the central composite RSM dataset (Table 3), the ANN was structured in a 3–X–1 topology, with a single hidden layer containing an optimised number of neurons. This architecture is consistent with findings that a single hidden layer with sufficient nodes can accurately approximate any continuous function (Cakir & Yilmaz, 2014; Xu et al., 2021).

The model was trained and validated using randomly divided training and testing subsets of the RSM dataset (Tables 5 and 6), and weights and biases were iteratively adjusted to minimise prediction error. The training process employed a sigmoid activation function in the hidden layer and a linear function at the output, which is suitable for regression tasks.

The optimal number of neurons in the hidden layer is typically determined through iterative experimentation, as no universal rule exists for all modelling scenarios. In this study, the neuron count was selected via a trial-and-error approach to achieve optimal network performance. Each neuron processes the input data and transmits it through synaptic weights along connecting pathways to subsequent layers (Kim et al., 1999). Insufficient neurons may constrain the model's capacity to learn complex patterns, whereas an excessive number may result in overfitting, where the network captures noise within the training data (Linko et al., 1999).

Previous studies have proposed various neuron ranges for hidden layers: Behera et al. (2015) recommended a range of 10 to 20 neurons for environmental datasets (Behera et al., 2015), while Oliveira et al. (2019) reported effective training performance within a narrower window of 3 to 10 neurons (Oliveira et al., 2019). In the present investigation, model accuracy was assessed using the coefficient of determination (R^2), with the highest value reaching 0.9998—indicating a near-perfect fit between the predicted and actual outcomes (Table 5). Accordingly, a network topology of 3 × 10 × 1 was selected as optimal. The model incorporated a sigmoid transfer function between the input and hidden layers, as well as between the hidden and output layers (Fig. 8), reinforcing its robustness in modelling Cr(VI) bioreduction by the strain MAHA-MIE.

Comparable findings have been reported in other domains. For instance, Jha and Sit (2021) applied a similar ANN configuration in their study on the supercritical fluid extraction of phytochemicals from Terminalia chebula pulp. Their optimal network architecture incorporated 10 neurons in the hidden layer, utilising sigmoid transfer functions between the input and hidden layers as well as between the hidden and output layers (Jha & Sit, 2021). Similarly, Hamidi et al. (2023) identified 10 hidden neurons as optimal for modelling Pb(II) removal using MMT K10 nanoclay, achieving a minimal mean squared error (MSE) of 0.0017 and a high coefficient of determination (R^2 = 0.9678) (Hamidi et al., 2023).

Table 5 Active Network Topology

Network	**Learning algorithm**	**Transfer function**		**Training dataset**		**Testing dataset**	
		Hidden layer	Output layer	R^2	RSME	R^2	RSME
3×7×1	BBP	Tanh	Tanh	0.9959	0.3735	0.9979	0.2730
3×8×1	IBP	Tanh	Linear	0.9958	0.4513	0.9989	0.1138

Journal of Chemical Health Risks
www.jchr.org
JCHR (2026) 16(1), 875-896 | ISSN:2251-6727

3×9×1	QP	Tanh	Threshold	0.9963	0.0958	0.9292	0.5656
3×10×1	BBP	Sigmoid	Sigmoid	0.9983	0.0138	0.9998	0.1419
3×15×1	GA	Sigmoid	Linear	0.9934	0.5261	0.9499	0.3351

BBP is Batch-backpropagation, IBP is Incremental Backpropagation, QP is Quick Prop, and GA is Genetic Algorithms.

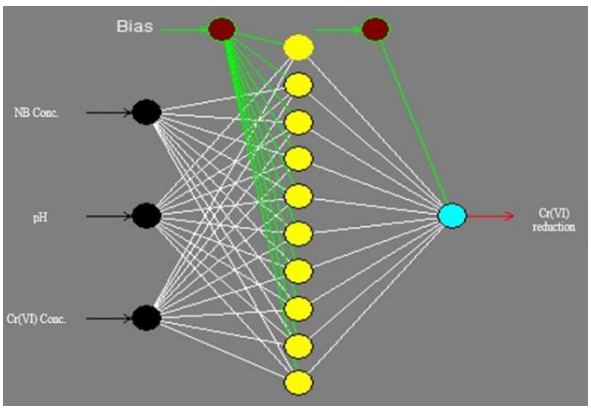

Fig. 8 Schematic representation of a (3×10×1) BBP-ANN.

3.8 Identification of Optimal Conditions via RSM and ANN Approaches

The identification and validation of optimal conditions between the RSM and ANN optimization techniques for free cells of *P. taichungensis* strain MAHA-MIE are presented in Table 6 In the RSM model, optimization is based on the desirability and priorities associated with each dependent and independent variable, where the desirability helps determine the most optimal conditions for responses (Amini & Younesi, 2009; Weaver et al., 2017). The numerical optimisation method, conducted using Design-Expert® software (version 13), yielded a desirability value of 1.0, indicating that the maximum Cr(VI) reduction rate achieved by free cells of *P. taichungensis* strain MAHA-MIE, as predicted by the RSM model, was 97.80% under optimized conditions comprising 9.49 g/L of nutrient broth, pH 6.48, and a Cr(VI) concentration of 50 ppm. The experimentally observed Cr(VI) reduction rate at this point was 96.72%.

Compared to the ANN model using Genetic Algorithm (GA), , an evolutionary optimization algorithm inspired by Darwinian natural selection and genetics. It searches for optimal solutions by simulating the process of natural evolution (Kumar et al., 2010). The experimental point for Cr(VI) reduction (99.17%) closely aligns with the predicted point (99.98%), resulting in a deviation of 0.81%. The optimized conditions were 9.56 g/L of nutrient broth, pH 6.48, and 69.57 ppm of Cr(VI) concentration. This suggests that the ANN model can be considered an appropriate model for predicting and optimizing for the prediction and optimization of Cr(VI) reduction by free cells of *P. taichungensis* strain MAHA-MIE. Similar findings indicated that the GA-ANN model provided a better fit and higher prediction accuracy (Soni et al., 2019; Yang et al., 2022).

Table 6 Comparison of the optimal conditions between RSM and ANN model

Model	**Algorithm**	**Nutrient broth conc. (g/L)**	**pH**	**Cr (VI) conc. (ppm)**	**Predicted point Cr (VI) reduction (%)**	**Experimental point Cr^{+6} reduction (%)**	**Deviation**
RSM	Desirability	9.49	6.48	50.03	97.80	96.72	1.2
ANN	Genetic algorithm	9.56	6.48	69.57	99.98	99.17	0.81

Journal of Chemical Health Risks
www.jchr.org
JCHR (2026) 16(1), 875-896 | ISSN:2251-6727

3.9 Three-Dimensional Surface Analysis via RSM and ANN Models

The three-dimensional (3D) response surface plots provide a graphical representation of the regression models, elucidating the relationships between the experimental response and each individual variable, as well as the nature of interactions between paired variables. These plots are colour-segmented, typically ranging from red (indicating regions of highest response intensity) through yellow and green to blue (representing the lowest response intensity) (Udeze et al., 2024). The influence of factors A (nutrient broth concentration), B (pH), and C (Cr(VI) concentration) on the dependent variable Y (Cr(VI) reduction) is clearly discernible through variations in gradient, contour density, and contour morphology within the 3D surface mappings (Ünsal et al., 2020). Fig. 9 and 10 (a, b, & c) depict the interactive effects of two independent variables on Cr(VI) reduction by free cells of strain MAHA-MIE, as modelled using RSM and ANN, respectively.

Fig. 9a and 10a demonstrate that Cr(VI) reduction is relatively low under acidic conditions but increases markedly as the pH approaches neutrality, reaching a maximum near pH 7.0. Fig. 9b and 10b show that increasing Cr(VI) concentrations result in a notable decline in reduction efficiency. However, elevated nutrient broth concentrations appear to attenuate this inhibitory effect, sustaining a comparatively high reduction rate. This suggests that sufficient nutrient availability is critical for maximising Cr(VI) reduction. Fig. 9c and 10c further reinforce the importance of pH, revealing that under lower Cr^{6+} concentrations, the reduction efficiency remains high across a broad pH spectrum.

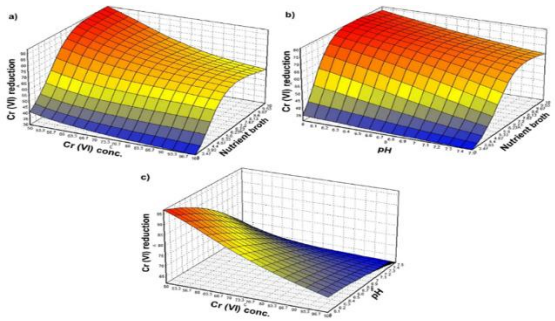

Fig. 9: Response surface graphs illustrating interaction factors by RSM.

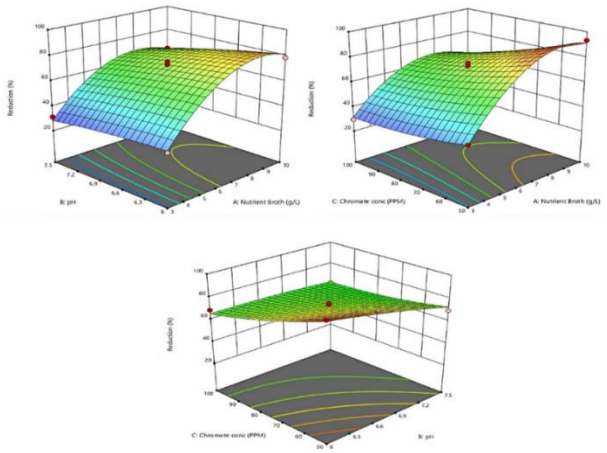

Figure 10 Response surface graphs illustrating interaction factors by ANN.

3.10 Comparative Analysis of RSM and ANN Modelling Approaches

To evaluate and compare the predictive performance of the Response Surface Methodology (RSM) and Artificial Neural Network (ANN) approaches, several statistical metrics were employed, including root mean square error (RMSE), coefficient of correlation (R^2), standard error of prediction (SEP), and relative percent deviation (RPD) (Aklilu et al., 2021). The lower values of RMSE, SEP, and RPD, together with higher R^2 values, indicate the accuracy and robustness of the predictive model (Choi et al., 2022). In this study, the ANN model outperformed the RSM model across all evaluation parameters, demonstrating superior predictive accuracy and model fit in forecasting Cr(VI) reduction efficiency by strain MAHA-MIE (Table 7).

Table 7 Comparison of statistical error metrics for RSM and ANN models

Model	Statistical parameters			
	RMSE	R^2	SEP (%)	RPD (%)
RSM	2.03	0.98	3.15	2.98
ANN	1.00	0.99	1.56	0.63

The strong performance of the ANN model can be attributed to its capacity to emulate biological neural networks, thereby enabling it to interpret the fundamental data structures and generalise complex

Journal of Chemical Health Risks
www.jchr.org
JCHR (2026) 16(1), 875-896 | ISSN:2251-6727

relationships between observed and predicted values (Praveen et al., 2021). Supporting evidence is provided by Vinayagam et al. (2022), who reported the effectiveness of ANN in modelling Cr(VI) biosorption using macroalgal spent biomass, as evidenced by the following comparative metrics: R^2_{RSM} = 0.9652, $RMSE_{RSM}$ = 0.8947, MAD_{RSM} = 4.0177 %, SPE_{RSM} = 1.83%, and R^2_{ANN} = 0.9998, $RMSE_{ANN}$ = 0.3986, MAD_{ANN} = 4.2636%, SEP_{ANN} = 0.81% (Vinayagam et al., 2022). Similarly, Ram Talib et al. (2019) reported that the ANN model as a superior and more accurate optimisation approach for Cr(VI) reduction by *Acinetobacter radioresistens* strain NS-MIE, as evidenced by the statistical metrics: R^2_{RSM} = 0.9974, $RMSE_{RSM}$ = 0.6781, RPD_{RSM} = 1.99 %, SPE_{RSM} = 2.19%, and R^2_{ANN} = 0.9991, $RMSE_{ANN}$ = 0.302, RPD_{ANN} = 2.57%, SEP_{ANN} = 0.33% (Ram Talib et al., 2019).

Figure 11 compares the regression models developed using RSM and ANN approaches. The ANN model yielded a higher coefficient of determination (R^2 = 0.99) than the RSM model (R^2 = 0.98), indicating superior predictive accuracy and reliability for estimating Cr(VI) reduction by strain MAHA-MIE. This enhanced performance underscores the ANN model's effectiveness in capturing the complex, nonlinear relationships inherent in the experimental data. In contrast, the RSM approach, being inherently polynomial, may exhibit limitations in modelling such intricacies (Banza et al., 2023).

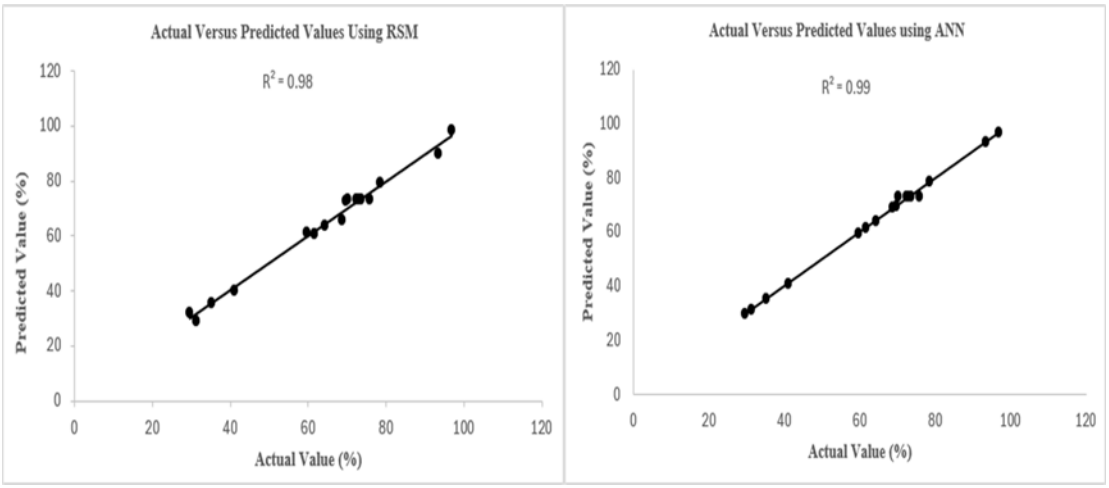

Figure 11 Actual versus RSM and ANN predicted values.

3.11 Studying the Effect of Cr(VI) on the Cellular Morphology of Free Cells of *P. taichungensis* strain MAHA-MIE Using Scanning Electron Microscopy (SEM)

The morphological tolerance ofnstrain MAHA-MIE to Cr(VI) was evaluated using SEM following exposure to 0, 50, and 100 ppm potassium dichromate ($K_2Cr_2O_7$) (Fig. 12a,b&c). In the absence of Cr(VI) (Figure 15a), the free cells displayed a characteristic rod-shaped morphology with smooth surfaces, uniform size distribution, and dense aggregation, features indicative of healthy physiological conditions. The absence of pronounced morphological distortions at 50 ppm Cr(VI) indicates that strain MAHA-MIE is capable of tolerating the toxicity of Cr(VI) exposure (Fig. 12b). In contrast, cells exposed to 100 ppm Cr(VI) exhibited pronounced morphological distortions. These included elongation, surface roughening, and irregular deformation (Figure 15c), implying significant structural stress and potential activation of adaptive defence mechanisms (Shen & Chou, 2016).

Despite these deformations, notable clustering of viable cells was still evident, underscoring a degree of resilience and tolerance to elevated Cr(VI) concentrations. This morphological adaptability parallels observations in *Bacillus licheniformis* SxR1, which, under 100 mg/L Cr(VI) exposure, transitioned from smooth, rod-like structures to roughened, elongated, and aggregated forms (Gupta et al., 2024). Similarly, *Pseudomonas aeruginosa* RW9 exhibited

Journal of Chemical Health Risks
www.jchr.org
JCHR (2026) 16(1), 875-896 | ISSN:2251-6727

comparable structural adaptations during Cr(VI) detoxification processes, further affirming that morphological plasticity is a common survival strategy among Cr(VI)-resistant bacterial taxa (Mat Arisah et al., 2021).

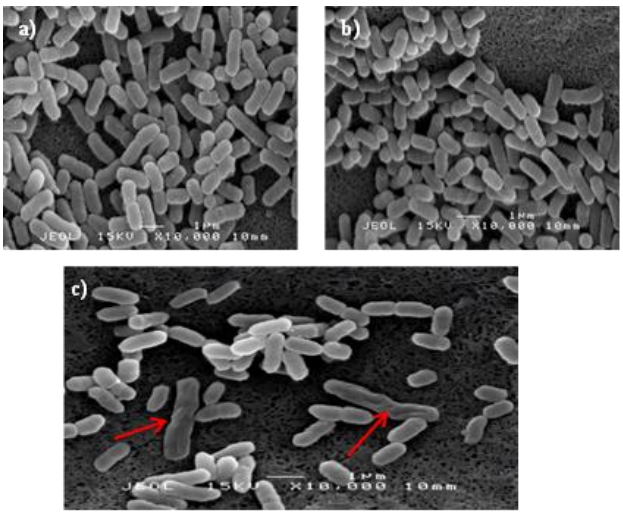

Fig. 12 SEM images of free cells of strain MAHA-MIE (a), control (b), at 50 ppm of $K_2Cr_2O_7$ (c), and at 100 ppm of $K_2Cr_2O_7$.

4 Conclusion

Among the thirty-one bacterial isolates screened, strain Cr-RB18 exhibited the highest Cr(VI) reduction efficiency, maintaining performance even at elevated Cr(VI) concentrations in nutrient broth (NB) after 24 hours of incubation. Biochemical characterisation identified the isolate as Gram-variable, facultatively anaerobic, motile, catalase-positive, and capable of both starch hydrolysis and H_2S production. Molecular identification further confirmed it as strain MAHA-MIE.

Under conditions optimised via artificial neural network (ANN) modelling, specifically, at a nutrient broth concentration of 9.56 g/L, pH 6.48, and Cr(VI) concentration of 69.57 ppm—the strain achieved a maximum Cr(VI) reduction efficiency of 99.17%. The ANN model demonstrated high predictive accuracy, with a coefficient of determination (R^2) of 0.99 and low associated error values (RMSE: 1.00; SEP: 1.56%; RPD: 0.63)

These results position strain MAHA-MIE as a promising biocatalyst for Cr(VI) bioremediation. Nevertheless, further investigation is warranted to elucidate its metabolic and regulatory mechanisms under both aerobic and anaerobic conditions, thereby enhancing its applicability in microbial biotechnology for the remediation of Cr(VI)-contaminated environments.

References

1. Abbas, A. T. (2023). *Laboratory Exercises in bacteriology*. https://www.researchgate.net/publication/368288436
2. Abdel-Fattah, Y. R., Saeed, H. M., Gohar, Y. M., & El-Baz, M. A. (2005). Improved production of Pseudomonas aeruginosa uricase by optimization of process parameters through statistical experimental designs. *Process Biochemistry*, *40*(5), 1707–1714.
3. Afshin, S., Rashtbari, Y., Vosough, M., Dargahi, A., Fazlzadeh, M., Behzad, A., & Yousefi, M. (2021). Application of Box–Behnken design for optimizing parameters of hexavalent chromium removal from aqueous solutions using Fe3O4 loaded on activated carbon prepared from alga: kinetics and equilibrium study. *Journal of Water Process Engineering*, *42*, 102113.
4. Ahmad, F. A., Yusuf, F., Shehu, U., Muhammad, F., & Yakasai, H. M. (2022). Isolation and identification of chromiumreducing bacteria from Challawa Industrial Area Kano State, Nigeria. *J. Adv. Microbiol*, *22*(1), 15–23.
5. Akhzari, F., Naseri, T., Mousavi, S. M., & Khosravi-Darani, K. (2024). A sustainable solution for alleviating hexavalent chromium from water streams using Lactococcus lactis AM99 as a novel Cr (VI)-reducing bacterium. *Journal of Environmental Management*, *353*, 120190.
6. Aklilu, E. G., Adem, A., Kasirajan, R., & Ahmed, Y. (2021). Artificial neural network and response surface methodology for modeling and optimization of activation of lactoperoxidase system. *South African Journal of Chemical Engineering*, *37*, 12–22.

Journal of Chemical Health Risks

www.jchr.org

JCHR (2026) 16(1), 875-896 | ISSN:2251-6727

7. Alam, G., Ihsanullah, I., Naushad, M., & Sillanpää, M. (2022). Applications of artificial intelligence in water treatment for optimization and automation of adsorption processes: Recent advances and prospects. *Chemical Engineering Journal*, *427*, 130011.
8. Amdoun, R., Khelifi, L., Khelifi-Slaoui, M., Amroune, S., Asch, M., Assaf-Ducrocq, C., & Gontier, E. (2010). Optimization of the culture medium composition to improve the production of hyoscyamine in elicited Datura stramonium L. hairy roots using the response surface methodology (RSM). *International Journal of Molecular Sciences*, *11*(11), 4726–4740.
9. AMELIA, T., LILIASARI, L., KUSNADI, K., & ADITIAWATI, P. (2023). Isolation and characterization of potential indigenous bacteria from the former bauxite mining area for heavy metal reduction. *Biodiversitas Journal of Biological Diversity*, *24*(9).
10. Amini, M., & Younesi, H. (2009). Biosorption of Cd (II), Ni (II) and Pb (II) from aqueous solution by dried biomass of Aspergillus niger: Application of response surface methodology to the optimization of process parameters. *CLEAN–Soil, Air, Water*, *37*(10), 776–786.
11. Anderson, A., Anbarasu, A., Pasupuleti, R. R., Manigandan, S., Praveenkumar, T. R., & Kumar, J. A. (2022). Treatment of heavy metals containing wastewater using biodegradable adsorbents: A review of mechanism and future trends. *Chemosphere*, *295*, 133724.
12. Banza, M., Seodigeng, T., & Rutto, H. (2023). Comparison study of ANFIS, ANN, and RSM and mechanistic modeling for chromium (VI) removal using modified cellulose nanocrystals–sodium alginate (CNC–alg). *Arabian Journal for Science and Engineering*, *48*(12), 16067–16085.
13. Bao, Z., Wang, X., Wang, Q., Zou, L., Peng, L., Li, L., Tu, W., & Li, Q. (2023). A novel method of domestication combined with ARTP to improve the reduction ability of Bacillus velezensis to Cr (VI). *Journal of Environmental Chemical Engineering*, *11*(1), 109091.
14. Baş, D., & Boyacı, İ. H. (2007). Modeling and optimization I: Usability of response surface methodology. *Journal of Food Engineering*, *78*(3), 836–845.
15. Bayatzadeh Fard, Z., Ghadimi, F., & Fattahi, H. (2017). Use of artificial intelligence techniques to predict distribution of heavy metals in groundwater of Lakan lead-zinc mine in Iran. *Journal of Mining and Environment*, *8*(1), 35–48.
16. Behera, S. K., Meher, S. K., & Park, H.-S. (2015). Artificial neural network model for predicting methane percentage in biogas recovered from a landfill upon injection of liquid organic waste. *Clean Technologies and Environmental Policy*, *17*, 443–453.
17. Bezerra, M. A., Santelli, R. E., Oliveira, E. P., Villar, L. S., & Escaleira, L. A. (2008). Response surface methodology (RSM) as a tool for optimization in analytical chemistry. In *Talanta* (Vol. 76, Issue 5, pp. 965–977). Elsevier. https://doi.org/10.1016/j.talanta.2008.05.019
18. Bharagava, R. N., & Mishra, S. (2018). Hexavalent chromium reduction potential of Cellulosimicrobium sp. isolated from common effluent treatment plant of tannery industries. *Ecotoxicology and Environmental Safety*, *147*, 102–109.
19. Box, G. E. P., & Behnken, D. W. (1960). Simplex-sum designs: a class of second order rotatable designs derivable from those of first order. *The Annals of Mathematical Statistics*, *31*(4), 838–864.
20. Buenaño, L., Ali, E., Jafer, A., Zaki, S. H., Hammady, F. J., Khayoun Alsaadi, S. B., Karim, M. M., Ramadan, M. F., Omran, A. A., & Alawadi, A. (2024). Optimization by Box–Behnken design for environmental contaminants removal using magnetic nanocomposite. *Scientific Reports*, *14*(1), 6950.
21. Cakir, L., & Yilmaz, N. (2014). Polynomials, radial basis functions and multilayer perceptron neural network methods in local

Journal of Chemical Health Risks

www.jchr.org

JCHR (2026) 16(1), 875-896 | ISSN:2251-6727

geoid determination with GPS/levelling. *Measurement*, *57*, 148–153.

22. Choi, H.-J., Naznin, M., Alam, M. B., Javed, A., Alshammari, F. H., Kim, S., & Lee, S.-H. (2022). Optimization of the extraction conditions of Nypa fruticans Wurmb. using response surface methodology and artificial neural network. *Food Chemistry*, *381*, 132086.
23. Dakiky, M., Khamis, M., Manassra, A., & Mer'Eb, M. (2002). Selective adsorption of chromium (VI) in industrial wastewater using low-cost abundantly available adsorbents. *Advances in Environmental Research*, *6*(4), 533–540.
24. Dbik, A., El Messaoudi, N., Bentahar, S., El Khomri, M., Lacherai, A., & Faska, N. (2022). Optimization of methylene blue adsorption on agricultural solid waste using box–behnken design (BBD) combined with response surface methodology (RSM) modeling. *Biointerface Res. Appl. Chem*, *12*(4), 4567–4583.
25. Dos Santos, H. R. M., Argolo, C. S., Argôlo-Filho, R. C., & Loguercio, L. L. (2019). A 16S rDNA PCR-based theoretical to actual delta approach on culturable mock communities revealed severe losses of diversity information. *BMC Microbiology*, *19*(1). https://doi.org/10.1186/s12866-019-1446-2
26. Elahi, A., Arooj, I., Bukhari, D. A., & Rehman, A. (2020). Successive use of microorganisms to remove chromium from wastewater. In *Applied Microbiology and Biotechnology* (Vol. 104, Issue 9, pp. 3729–3743). Springer. https://doi.org/10.1007/s00253-020-10533-y
27. Fan, M., Hu, J., Cao, R., Ruan, W., & Wei, X. (2018). A review on experimental design for pollutants removal in water treatment with the aid of artificial intelligence. *Chemosphere*, *200*, 330–343.
28. Farag, S., & Zaki, S. (2010). Identification of bacterial strains from tannery effluent and reduction of hexavalent chromium. *Journal of Environmental Biology*, *31*(5), 877.
29. Firdausi, A. N., Aminah, A., & Setyawati, I. (2024). UTILIZATION OF SOYBEAN POWDER AS AN ALTERNATIVE MEDIA FOR THE GROWTH OF ANAEROBIC BACTERIA. *Dentino: Jurnal Kedokteran Gigi*, *9*(2), 218–223.
30. Fito, J., Tibebu, S., & Nkambule, T. T. I. (2023). Optimization of Cr (VI) removal from aqueous solution with activated carbon derived from Eichhornia crassipes under response surface methodology. *BMC Chemistry*, *17*(1), 4.
31. Gendy, T. S., Zakhary, A. S., & Ghoneim, S. A. (2021). Response surface methodology and artificial neural network methods comparative assessment for fuel rich and fuel lean catalytic combustion. *World Journal of Engineering and Technology*, *9*(4), 816–847.
32. Ghorbani, F., Kamari, S., Zamani, S., Akbari, S., & Salehi, M. (2020). Optimization and modeling of aqueous Cr (VI) adsorption onto activated carbon prepared from sugar beet bagasse agricultural waste by application of response surface methodology. *Surfaces and Interfaces*, *18*, 100444.
33. Guo, Y., Deng, J., Ren, Z., Huang, Z., Wei, C., & Huang, M. (2021). *Optimization of the production of ethyl hexanoate and ethyl butyrate by cofermentation of Saccharomyces cerevisiae and esterifying bacteria from pit mud of Chinese Baijiu using response surface methodology.*
34. Gupta, A., Gond, S. K., & Mishra, V. K. (2024). Isolation and characterization of hexavalent chromium-tolerant endophytic bacteria inhabiting Solanum virginicum L. roots: A study on potential for chromium bioremediation and plant growth promotion. *Journal of Hazardous Materials Letters*, 100114.
35. Gurney, K. (2018). *An introduction to neural networks*. CRC press.
36. Hamidi, F., Baghani, A. N., Kasraee, M., Salari, M., & Mehdinejad, M. H. (2023). Modeling, optimization and efficient use of MMT K10 nanoclay for Pb (II) removal using RSM, ANN and GA. *Scientific Reports*,

Journal of Chemical Health Risks

www.jchr.org

JCHR (2026) 16(1), 875-896 | ISSN:2251-6727

13(1). https://doi.org/10.1038/s41598-023-35709-0

37. Heuer, H., Krsek, M., Baker, P., Smalla, K., & Wellington, E. M. H. (1997). Analysis of Actinomycete Communities by Specific Amplification of Genes Encoding 16S rRNA and Gel-Electrophoretic Separation in Denaturing Gradients. In *APPLIED AND ENVIRONMENTAL MICROBIOLOGY* (Vol. 63, Issue 8). https://journals.asm.org/journal/aem
38. Huang, Y., Tang, J., Zhang, B., Long, Z.-E., Ni, H., Fu, X., & Zou, L. (2023). Influencing factors and mechanism of Cr (VI) reduction by facultative anaerobic Exiguobacterium sp. PY14. *Frontiers in Microbiology*, *14*, 1242410.
39. Huang, Y., Zeng, Q., Hu, L., Xiong, D., Zhong, H., & He, Z. (2021). Column study of enhanced Cr (VI) removal and removal mechanisms by Sporosarcina saromensis W5 assisted bio-permeable reactive barrier. *Journal of Hazardous Materials*, *405*, 124115.
40. Hussain, S., Maqbool, Z., Shahid, M., Shahzad, T., Muzammil, S., Zubair, M., Iqbal, M., Ahmad, I., Imran, M., & Ibrahim, M. (2020). *Simultaneous removal of reactive dyes and hexavalent chromium by a metal tolerant Pseudomonas sp. WS-D/183 harboring plant growth promoting traits.*
41. Ikegami, K., Hirose, Y., Sakashita, H., Maruyama, R., & Sugiyama, T. (2020). Role of polyphenol in sugarcane molasses as a nutrient for hexavalent chromium bioremediation using bacteria. *Chemosphere*, *250*, 126267. https://doi.org/10.1016/j.chemosphere.2020.126267
42. Jha, A. K., & Sit, N. (2021). Comparison of response surface methodology (RSM) and artificial neural network (ANN) modelling for supercritical fluid extraction of phytochemicals from Terminalia chebula pulp and optimization using RSM coupled with desirability function (DF) and genetic algorithm (GA) and ANN with GA. *Industrial Crops and Products*, *170*, 113769.
43. Jobby, R., Jha, P., Yadav, A. K., & Desai, N. (2018). Biosorption and biotransformation of hexavalent chromium [Cr (VI)]: a comprehensive review. *Chemosphere*, *207*, 255–266.
44. Kalsoom, A., Batool, R., & Jamil, N. (2021). Highly Cr(vi)-tolerant Staphylococcus simulans assisting chromate evacuation from tannery effluent. *Green Processing and Synthesis*, *10*(1), 295–308. https://doi.org/10.1515/gps-2021-0027
45. Kao, C.-M., Chen, S.-C., Liao, Z.-Y., Wen, S.-S., & Chien, C.-C. (2021). Characterization of two chromate reducing bacteria isolated from heavy metal contaminated soil. *Biologia*, *76*, 3909–3917.
46. Khanam, R., Al Ashik, S. A., Suriea, U., & Mahmud, S. (2024). Isolation of chromium resistant bacteria from tannery waste and assessment of their chromium reducing capabilities – A Bioremediation Approach. *Heliyon*, *10*(6). https://doi.org/10.1016/j.heliyon.2024.e27821
47. Kim, D. H., Kim, D. J., & Kim, B. M. (1999). The application of neural networks and statistical methods to process design in metal forming processes. *The International Journal of Advanced Manufacturing Technology*, *15*(12), 886–894.
48. Kothari, M. S., Vegad, K. G., Shah, K. A., & Hassan, A. A. (2022). An artificial neural network combined with response surface methodology approach for modelling and optimization of the electro-coagulation for cationic dye. *Heliyon*, *8*(1).
49. Kumar, M., Husain, D. M., Upreti, N., & Gupta, D. (2010). Genetic algorithm: Review and application. *Available at SSRN 3529843*.
50. Lakshmi, D., Akhil, D., Kartik, A., Gopinath, K. P., Arun, J., Bhatnagar, A., Rinklebe, J., Kim, W., & Muthusamy, G. (2021). Artificial intelligence (AI) applications in adsorption of heavy metals using modified biochar. *Science of the Total Environment*, *801*, 149623.

Journal of Chemical Health Risks

www.jchr.org

JCHR (2026) 16(1), 875-896 | ISSN:2251-6727

51. Lee, F. L., Tien, C. J., Tai, C. J., Wang, L. T., Liu, Y. C., & Chern, L. L. (2008). Paenibacillus taichungensis sp. nov., from soil in Taiwan. *International Journal of Systematic and Evolutionary Microbiology*, *58*(11), 2640–2645. https://doi.org/10.1099/ijs.0.65776-0
52. Linko, S., Zhu, Y.-H., & Linko, P. (1999). Applying neural networks as software sensors for enzyme engineering. *Trends in Biotechnology*, *17*(4), 155–162.
53. Madhavi, V., Reddy, A. V. B., Reddy, K. G., Madhavi, G., & Prasad, T. (2013). An overview on research trends in remediation of chromium. *Research Journal of Recent Sciences*, *2277*, 2502.
54. Manohar, B., & Divakar, S. (2005). An artificial neural network analysis of porcine pancreas lipase catalysed esterification of anthranilic acid with methanol. *Process Biochemistry*, *40*(10), 3372–3376.
55. Masi, C., Gemechu, G., & Tafesse, M. (2021). Isolation, screening, characterization, and identification of alkaline protease-producing bacteria from leather industry effluent. *Annals of Microbiology*, *71*, 1–11.
56. Mat Arisah, F., Amir, A. F., Ramli, N., Ariffin, H., Maeda, T., Hassan, M. A., & Mohd Yusoff, M. Z. (2021). Bacterial resistance against heavy metals in Pseudomonas aeruginosa RW9 involving hexavalent chromium removal. *Sustainability*, *13*(17), 9797.
57. Maurya, A., Kumar, P. S., & Raj, A. (2022). Characterization of biofilm formation and reduction of hexavalent chromium by bacteria isolated from tannery sludge. *Chemosphere*, *286*. https://doi.org/10.1016/j.chemosphere.2021.131795
58. McLean, J. S., Beveridge, T. J., & Phipps, D. (2000). Isolation and characterization of a chromium-reducing bacterium from a chromated copper arsenate-contaminated site. *Environmental Microbiology*, *2*(6), 611–619.
59. Meng, Y., Ma, X., Luan, F., Zhao, Z., Li, Y., Xiao, X., Wang, Q., Zhang, J., & Thandar, S. M. (2022). Sustainable enhancement of Cr (VI) bioreduction by the isolated Cr (VI)-resistant bacteria. *Science of The Total Environment*, *812*, 152433.
60. Mishra, S., Chen, S., Saratale, G. D., Saratale, R. G., Romanholo Ferreira, L. F., Bilal, M., & Bharagava, R. N. (2021). Reduction of hexavalent chromium by Microbacterium paraoxydans isolated from tannery wastewater and characterization of its reduced products. *Journal of Water Process Engineering*, *39*. https://doi.org/10.1016/j.jwpe.2020.101748
61. Mohammadi, A., Nemati, S., Mosaferi, M., Abdollahnejhad, A., Almasian, M., & Sheikhmohammadi, A. (2017). Predicting the capability of carboxymethyl cellulose-stabilized iron nanoparticles for the remediation of arsenite from water using the response surface methodology (RSM) model: modeling and optimization. *Journal of Contaminant Hydrology*, *203*, 85–92.
62. Mustapha, M. U., & Halimoon, N. (2015). Screening and isolation of heavy metal tolerant bacteria in industrial effluent. *Procedia Environmental Sciences*, *30*, 33–37.
63. Nabavi-Pelesaraei, A., Bayat, R., Hosseinzadeh-Bandbafha, H., Afrasyabi, H., & Berrada, A. (2017). Prognostication of energy use and environmental impacts for recycle system of municipal solid waste management. *Journal of Cleaner Production*, *154*, 602–613.
64. Nacer, A., Boudjema, S., Bouhaous, M., Boudouaia, N., & Bengharez, Z. (2021). Bioremediation of hexavalent chromium by an indigenous bacterium Bacillus cereus S10C1: optimization study using two level full factorial experimental design. *Comptes Rendus. Chimie*, *24*(S1), 57–70.
65. Narayani, M., & Shetty, K. V. (2013). Chromium-resistant bacteria and their environmental condition for hexavalent chromium removal: a review. *Critical*

Reviews in Environmental Science and Technology, *43*(9), 955–1009.

66. Navarrete-Perea, J., Gygi, S. P., & Paulo, J. A. (2021). Growth media selection alters the proteome profiles of three model microorganisms. *Journal of Proteomics*, *231*, 104006.
67. Newsome, L., & Falagán, C. (2021). The microbiology of metal mine waste: Bioremediation applications and implications for planetary health. *GeoHealth*, *5*(10), e2020GH000380.
68. Oliveira, V., Sousa, V., & Dias-Ferreira, C. (2019). Artificial neural network modelling of the amount of separately-collected household packaging waste. *Journal of Cleaner Production*, *210*, 401–409.
69. Prashanthi, R., Shreevatsa, G. K., Krupalini, S., & Manoj, L. (2021). Isolation, characterization, and molecular identification of soil bacteria showing antibacterial activity against human pathogenic bacteria. *Journal of Genetic Engineering and Biotechnology*, *19*(1), 120.
70. Praveen, S., Jegan, J., Pushpa, T. B., & Gokulan, R. (2021). Artificial neural network modelling for biodecolorization of Basic Violet 03 from aqueous solution by biochar derived from agro-bio waste of groundnut hull: kinetics and thermodynamics. *Chemosphere*, *276*, 130191.
71. Ram Talib, N. S., Halmi, M. I. E., Abd Ghani, S. S., Zaidan, U. H., & Shukor, M. Y. A. (2019). Artificial neural networks (ANNs) and response surface methodology (RSM) approach for modelling the optimization of chromium (VI) reduction by newly isolated Acinetobacter radioresistens strain NS-MIE from agricultural soil. *BioMed Research International*, *2019*.
72. Rath, B. P., Das, S., Mohapatra, P. K. Das, & Thatoi, H. (2014). Optimization of extracellular chromate reductase production by Bacillus amyloliquefaciens (CSB 9) isolated from chromite mine environment. *Biocatalysis and Agricultural Biotechnology*, *3*(3), 35–41.
73. Saber, W. I. A., Ghoniem, A. A., Al-Otibi, F. O., El-Hersh, M. S., Eldadamony, N. M., Menaa, F., & Elattar, K. M. (2023). A comparative study using response surface methodology and artificial neural network towards optimized production of melanin by Aureobasidium pullulans AKW. *Scientific Reports*, *13*(1), 13545.
74. Sadhana Sagar, S. S., Abhishek Dwivedi, A. D., Suneel Yadav, S. Y., Manishi Tripathi, M. T., & Kaistha, S. D. (2012). *Hexavalent chromium reduction and plant growth promotion by Staphylococcusarlettae Strain Cr11.*
75. Sanjay, M. S., Sudarsanam, D., Raj, G. A., & Baskar, K. (2020). Isolation and identification of chromium reducing bacteria from tannery effluent. *Journal of King Saud University - Science*, *32*(1), 265–271. https://doi.org/10.1016/j.jksus.2018.05.001
76. Shen, J.-P., & Chou, C.-F. (2016). Morphological plasticity of bacteria—Open questions. *Biomicrofluidics*, *10*(3).
77. Shet, V. B., Palan, A. M., Rao, S. U., Varun, C., Aishwarya, U., Raja, S., Goveas, L. C., Vaman Rao, C., & Ujwal, P. (2018). Comparison of response surface methodology and artificial neural network to enhance the release of reducing sugars from non-edible seed cake by autoclave assisted HCl hydrolysis. *3 Biotech*, *8*(2), 127.
78. Soni, U., Roy, A., Verma, A., & Jain, V. (2019). Forecasting municipal solid waste generation using artificial intelligence models—a case study in India. *SN Applied Sciences*, *1*(2), 162.
79. Sopian, N. A., Halmi, M. I. E., Abd Shukor, M. Y., Sabullah, M. K., & Johari, W. L. W. (2014). Isolation, characterization and growth optimization of a chromate-reducing bacterium. *Bioremediation Science and Technology Research*, *2*(2), 18–24.
80. Tan, H., Wang, C., Zeng, G., Luo, Y., Li, H., & Xu, H. (2020). Bioreduction and biosorption of Cr (VI) by a novel Bacillus sp. CRB-B1 strain. *Journal of Hazardous Materials*, *386*, 121628.

81. Teófilo, R. F., & Ferreira, M. (2006). Chemometrics II: spreadsheets for experimental design calculations, a tutorial. *Química Nova*, *29*, 338–350.
82. Udeze, O. J., Mohammed, B. S., Adebanjo, A. U., & Abdulkadir, I. (2024). Optimizing an eco-friendly high-density concrete for offshore applications: A study on fly ash partial replacement and graphene oxide nano reinforcement. *Case Studies in Chemical and Environmental Engineering*, *9*, 100592.
83. Ukhurebor, K. E., Aigbe, U. O., Onyancha, R. B., Nwankwo, W., Osibote, O. A., Paumo, H. K., Ama, O. M., Adetunji, C. O., & Siloko, I. U. (2021). Effect of hexavalent chromium on the environment and removal techniques: a review. *Journal of Environmental Management*, *280*, 111809.
84. Ünsal, M., Işık-Gülsaç, I., Üresin, E., Budak, M. S., Özgür-Büyüksakallı, K., Sayar, A., Aksoy, P., Ünlü, N., Okur, O., & Şahin, H. (2020). Optimisation of biomass catalytic depolymerisation conditions by using response surface methodology. *Waste Management & Research*, *38*(3), 322–331.
85. Vinayagam, R., Dave, N., Varadavenkatesan, T., Rajamohan, N., Sillanpää, M., Nadda, A. K., Govarthanan, M., & Selvaraj, R. (2022). Artificial neural network and statistical modelling of biosorptive removal of hexavalent chromium using macroalgal spent biomass. *Chemosphere*, *296*, 133965.
86. Weaver, K. F., Morales, V. C., Dunn, S. L., Godde, K., & Weaver, P. F. (2017). *An introduction to statistical analysis in research: with applications in the biological and life sciences*. John Wiley & Sons.
87. Wei, Y., Usman, M., Farooq, M., Adeel, M., Haider, F. U., Pan, Z., Chen, W., Liu, H., & Cai, L. (2022). Removing hexavalent chromium by nano zero-valent iron loaded on attapulgite. *Water, Air, & Soil Pollution*, *233*(2), 48.
88. Xu, A., Chang, H., Xu, Y., Li, R., Li, X., & Zhao, Y. (2021). Applying artificial neural networks (ANNs) to solve solid waste-related issues: A critical review. *Waste Management*, *124*, 385–402.
89. Yang, T., Lai, H., Cao, Z., Niu, Y., Xiang, J., Zhang, C., & Shang, L. (2022). Comparison of an Artificial Neural Network and a Response Surface Model during the Extraction of Selenium-Containing Protein from Selenium-Enriched Brassica napus L. *Foods*, *11*(23), 3823.
90. Yu, Y., Ali, J., Yang, Y., Kuang, P., Zhang, W., Lu, Y., & Li, Y. (2022). Synchronous Cr (VI) remediation and energy production using microbial fuel cell from a subsurface environment: A review. *Energies*, *15*(6), 1989.
91. Zaib, Q., & Ahmad, F. (2020). Experimental modeling to optimize the sonication energy in water. *Measurement*, *163*, 108039.
92. Zeng, W., Li, F., Wu, C., Yu, R., Wu, X., Shen, L., Liu, Y., Qiu, G., & Li, J. (2020). Role of extracellular polymeric substance (EPS) in toxicity response of soil bacteria Bacillus sp. S3 to multiple heavy metals. *Bioprocess and Biosystems Engineering*, *43*, 153–167.